East European Journal of Physics. **2.** 321-326 (2024)
DOI:10.26565/2312-4334-2024-2-37 ISSN 2312-4334

EFFECT OF γ-IRRADIATION ON STRUCTURE AND ELECTROPHYSICAL PROPERTIES OF S-DOPED ZnO FILMS

Sirajidin S. Zainabidinov[a], Akramjon Y. Boboev[a,b]*, Nuritdin Y. Yunusaliyev[a]
[a]*Andijan state university named after Z.M. Babur, Andijan, Uzbekistan*
[b]*Institute of Semiconductor Physics and Microelectronics at the National University of Uzbekistan, 20 Yangi Almazar st., Tashkent, 100057, Uzbekistan*
**Corresponding Author e-mail: aboboevscp@gmail.com*
Received March 11, 2024; revised April 8, 2024; accepted April 26, 2024

The produced *ZnO<S>* films were characterized with the crystallographic orientation (*001*) and lattice parameters $a = b = 0.3265$ nm and $c = 0.5212$ nm. $ZnO_{1-x}S_x$ nano-crystallites on the surface of the film had characteristic sizes ranging from 50 nm to 200 nm. The lattice parameter of $ZnO_{1-x}S_x$ nano-crystallites was experimentally determined to be $a_{ZnO<S>} = 0.7598$ nm. The study has shed light on what occurs to lattice parameters of the *ZnO* film and the geometric dimensions of $ZnO_{1-x}S_x$ nano-crystallites on the surface of the film under the influence of gamma-irradiation. It has been determined that the crystal structure of $ZnO_{1-x}S_x$ nanocrystallites represents a cubic lattice and belongs to the space group *F43m*. It has been determined that after γ-irradiation at doses $5 \cdot 10^6$ *rad*, the resistivity of *ZnO<S>* films reduced to $\rho = 12{,}7$ *Ω·cm* and the mobility of the majority charge carriers (μ) became $0.18\ cm^2/V \cdot s$, whereas their concentration (N) had increased and equaled $2.64 \cdot 10^{18}\ cm^{-3}$. The study of the current-voltage characteristics of *p- ZnO<S>/n-Si* heterostructures before and after γ-irradiation at doses of $5 \cdot 10^6$ *rad* revealed that the dependence of the current on voltage obeys an exponential law which is consistent with the theory of the injection depletion phenomenon. It was determined that under the influence of γ-irradiation at doses of $5 \cdot 10^6$ *rad*, the capacitance of the *p-ZnO<S>/n-Si* heterostructure at negative voltages increases and the shelved curve sections and peaks are observed on the curve due to the presence of a monoenergetic level of fast surface states at the heterojunction.
Keywords: *Film; Ultrasonic spray pyrolysis; Nano-crystallite; γ-irradiation; Crystallographic orientation; Lattice parameter; Charge carriers; Injection depletion*
PACS: 78.30.Am

INTRODUCTION

ZnO metal oxide layers represent semiconductors with a band gap of *3.3eV* and *n*-type conductivity due to oxygen deficiency [1]. The layers are conventionally engineered by three most promising techniques such as, synthesis and doping of zinc oxide under substantially non-equilibrium conditions; thermal annealing under a film of substance with inadequate solubility of the components of compounds; annealing of crystals in an atmosphere of atomic chalcogen [2,3]. In the present experimental case, to a certain extent, all three of these approaches have been implemented. Thus, in the process of pyrolysis of ultrathin films of zinc nitrates and/or acetates solutions, significantly non-equilibrium thermodynamic conditions occur on the surface of the substrate leading to the formation of atomic oxygen and sulfur, as well as *O-S, Zn-O-S* groups, etc., that further line up in a growing film [4]. By applying (choosing) substrates with various solubilities (or different diffusion coefficients) of *Zn, O* and *S* atoms, it would be possible, during post-growth annealing, to optimize the relative rates of "healing" of various defects. In addition, as was revealed earlier, doping metal oxide layers with various elements [5] and their subsequent exposure to γ-irradiation [6,7] leads to a reduction in size of crystallite grains and boosts functional properties of nanostructured films.

In this regard, the paper presents the results of experimental studies of *XRD* (X-ray diffraction analysis) and electrophysical properties of *ZnO* metal oxide films doped with *S*, as well as the effect of γ-irradiation on their structural parameters.

MATERIALS AND METHODS

To deposit *S*-doped *ZnO* metal oxide films on silicon substrates, we used the technique of ultrasonic spray pyrolysis.

X-ray diffraction analysis of the resulting thin *ZnO<S>* films and silicon substrates were performed by a third-generation Empyrean Malvern-multipurpose X-ray diffractometer. OriginPro2019 package was used to analyze the correspondent spectra. X-ray diffraction measurements were carried out in the Bragg–Brentano beam geometry in the range $2\theta_B$ = from *15°* to *120°* continuously with a scanning speed of *1 degree/min*.

To determine the resistivity, concentration and the mobility of the majority charge carriers in the grown films, the Van der Pauw method was used on a *HMS-7000* Hall effect measurement unit.

RESULTS AND DISCUSSION

Figure 1-a shows an XRD pattern of the received *ZnO<S>* metal oxide layer. It is clear from the X-ray diffraction patterns of *ZnO<S>* films that their surface corresponds to the crystallographic orientation *(001)* and differs significantly from the X-ray diffraction pattern of the silicon substrate.

Cite as: S.S. Zainabidinov, A.Y. Boboev, N.Y. Yunusaliyev, East Eur. J. Phys. 2, 321 (2024), https://doi.org/10.26565/2312-4334-2024-2-37

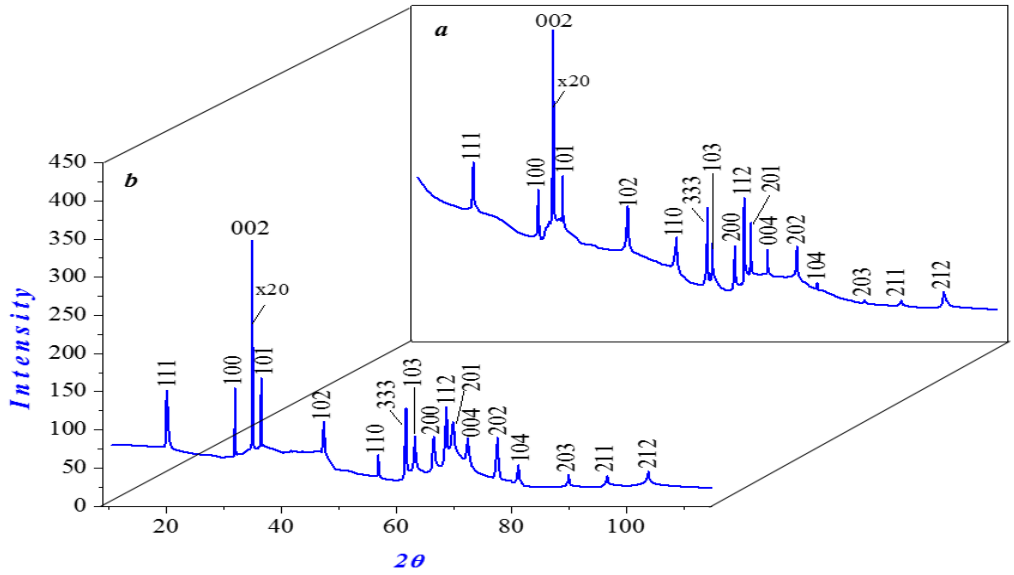

Figure 1. X-ray diffraction patterns of ZnO<S> films before (*a*) and after gamma irradiation (*b*)

The above results are indicative of change in the crystal lattice of the matrix layer. The values of the lattice parameters from these reflections (002) were determined to be following: $a = b = 0.3265$ nm and $c = 0.5212$ nm. Tentative analysis and the study of this reflection showed that it most probably belongs to the space group $P6_3mc$ and has a hexagonal system in the crystal lattice. In addition, other structural reflections with different orientations were observed in the *XRD* pattern (Fig. *1-a*.), and their diffraction characteristics are presented hereunder in Table 1.

Table 1. Diffraction characteristics of the ZnO-S/Si system before and after γ-irradiation at doses of $5 \cdot 10^6$ rad

№	Reflection [2]	ZnO-S/Si		γ-ZnO-S/Si		ΔΘ
		I	2Θ,	I	2Θ,	
1	111	239	20.081	150.9	20.1	0.019
2	100	203	31.86	72	31.79	0.07
3	002	416.63	34.19	264	34.29	0.1
4	101	214.15	35.93	168.3	36	0.07
5	102	181.45	47.45	103.6	47.47	0.02
6	110	124.8	56.79	66.6	56.87	0.08
7	333	179	61.61	128.9	61.68	0.07
8	103	131	62.53	91.6	62.64	0.11
9	200	117.6	66.42	90.6	66.49	0.07
10	112	192	68.59	109.5	68.68	0.09
11	201	159	69.31	110	69.37	0.06
12	004	123	72.28	88.5	72.31	0.03
13	202	127.7	77.5	89.4	77.6	0.1
14	104	79	81.2	54	81.23	0.03
15	203	55.8	89.49	41	89.59	0.1
16	211	55.3	96.35	39.7	96.4	0.05
17	212	66	103.56	45.2	103.66	0.1

Also, at smaller and medium scattering angles of *XRD* pattern, an inelastic background reflection was observed, associated with the appearance of micro size distortions of the crystal lattice of the film, caused by the mismatch of lattice constants of the matrix layer and the substrate, determined from the following expression [8, 9]:

$$\xi = 2\left|a_{M.C} - a_{П}\right| / \left(a_{M.C} + a_{П}\right), \tag{1}$$

In this case, the mismatch of lattice constants was equal to 0.02, i.e. the lattice mismatch of the *ZnO-S/Si (100)* system happens to be 2%. The existence of various type of micro-size distortions of the crystal lattice leads to the formation of nanoobjects in the near-surface regions of the film [10, 11].

That nanosized assemblies are being shaped in the crystal lattice is proven by the appearance of structural lines (*111*) and (*333*). They belong to $ZnO_{1-x}S_x$ nano-crystallites. The sizes of nano-crystallites were determined from the half-width of these reflections using the following expression [12,13]:

Reflection (X-ray structural analysis) is a peak in an X-ray pattern corresponding to Bragg reflection from one of the crystallographic planes. Characterized by Miller indices.

$$D = K\lambda / (\beta \cos\theta) , \tag{2}$$

where λ is irradiation wavelength, (λ = *0.154 nm*), θ is the scattering angle (half the diffraction angle $2\theta_Б$), β - physical broadening of the line in the diffraction pattern (reflection width at half maximum intensity) in radians, coefficient $K \approx 0.94$ [8].

$$\beta = \frac{1}{2}(B - b + \sqrt{B(B-b)} , \tag{3}$$

where B represents true broadening of the reflection, b is the true geometric broadening of the reflection [8].

Calculations of D values using the given formula (2) showed that the size of $ZnO_{1-x}S_x$ nano-crystallites ranges from 50 nm to 200 nm. The lattice parameter $a_{ZnO<S>}$ of $ZnO_{1-x}S_x$ nano-crystallites was experimentally determined 0.7598 nm.

Figure 1-*b* shows an *XRD* pattern of a *ZnO<S>* film after *γ*-irradiation at doses of $5 \cdot 10^6$ *rad*. It differs from *XRD* pattern of the *ZnO<S>* film before irradiation; in it one can see that the level of inelastic background reflection decreases by 72% at smaller and medium angles, as well as a decrease in the intensity of the main reflection (*002*) by 13.8% as well as its further shift towards large scattering angles (Fig. 1-*b*). In addition, the authors determined the values of the lattice parameters of the *ZnO<S>* film based on the experimental data of the main reflection (*002*), which were $a = b = 0.3246$ nm and $c = 0.5187$ nm, i.e. slightly less than the lattice parameter of the *ZnO<S>* film before irradiation ($a = b = 0.3265$ nm and $c = 0.5256$ nm). These observed effects indicate that nano-crystallites of $ZnO_{1-x}S_x$-type gather locally and might be associated with a uniform distribution on the surface of the film and prove the presence of several diffraction reflections on the X-ray diffraction pattern, given in Table 1.

As Table 1 and Fig. 1*b* clearly show, the X-ray diffraction pattern demonstrates a decrease in intensities and half-widths of other diffraction reflections and a shift towards larger scattering angles. This is indicative of a decrease in the lattice parameters of the *ZnO* film and the geometric dimensions of $ZnO_{1-x}S_x$ nano-crystallites on the film surface. The authors analyzed the experimental results of these reflections and determined that the crystal structure of $ZnO_{1-x}S_x$ nano-crystallites corresponds to a cubic lattice belonging to the space group *F43m*. The cubic lattice parameter of the nano-crystallites was also determined from the observed reflections, which is approximately 0.7692 nm. The average size of $ZnO_{1-x}S_x$ nano-crystallites (D) was calculated in formula (2) using X-ray diffraction data, which were in the range of 10÷150 nm.

The results show that the electrical properties of *p-ZnO<S>* films do indeed improve after irradiation. Before irradiation, these parameters were as follows: resistivity $\rho = 16.2$ *Ω·cm*, concentration $N = 1.83 \cdot 10^{18}$ *cm*$^{-3}$ and the mobility of the majority charge carriers at room temperature $\mu = 0.31$ *cm*^{2}*/V·s*. After *γ*-irradiation at doses of $5 \cdot 10^6$ *rad,* resistivity ρ of the samples turned out to be *12.7 Ω·cm* whereas the mobility of the majority charge carriers $\mu = 0.18$ *cm*^{2}*/V·s* of *ZnO<S>* films had decreased, while their concentration appeared to increase $N = 2.64 \cdot 10^{18}$ *cm*$^{-3}$. In [14] the authors claim they have witnessed a decrease in the size of nano-crystallites of *ZnO* films with *Al* atoms and a decrease in the mobility of the majority charge carriers. According to X-ray diffraction and electron microscopy analysis of *ZnO<S>* films, after *γ*-irradiation, the size of nano-crystallites used to decrease. A decrease in the size of nano-crystallites leads to an increase in the number of boundaries (edges) in them and thus, to a further decrease in the electron mean free path [15]. This, in turn, leads to a decrease in the mobility of the majority charge carriers.

The current-voltage characteristic was measured using a standard method using a probe at room temperature. We used a DC Power Supply stabilized voltage source *HY3005*, a *MASTECH M3900* digital multimeter in ammeter and voltmeter modes.

To understand the mechanism of the transfer of electric current, the current-voltage (CV) and capacitance-voltage (CV) curves of the fabricated *p-ZnO<S>/n-Si* heterostructures were studied before and after γ-irradiation. Figure 2 shows the forward bias of current-voltage characteristics of *p-ZnO<S>/n-Si* heterostructures consisting of two sections. From Figure *2a* it can be seen that the dependence of current on voltage obeys an exponential law, regardless of irradiation, described in [16-18]:

$$I = I_o \exp(eU/ckT), \tag{4}$$

where I_0 is the pre-exponential factor ($I_0 = 2.6 \cdot 10^{-6}$ A), e-elementary charge (~$1.6 \cdot 10^{-19}$ C), U-the voltage applied, k - Boltzmann constant, T-temperature. The coefficient c in the denominator of the exponent is determined using the following expression based on two consecutive experimental results:

$$c = e(U_2 - U_1)/kT\ln(I_2/I_1), \tag{5}$$

which was 7.84.

The next ascending trend in the «*current versus voltage*» curve is observed in sublinear region of the current-voltage characteristic of *p-ZnO<S>/n-Si* heterostructure (Fig. *2b*) which is explained by the phenomenon of injection depletion [19] and is expressed by the following analytical relationship:

$$U \approx U_0 \exp(jad), \tag{6}$$

here U_0 is the voltage of the beginning of the sublinear section of the current-voltage curve, j is the current density, d is the length of the base region, a is the constant determined by the following expression [20]:

$$a = \left(2eD_pN_t\right)^{-1}, \tag{7}$$

here D_p is the diffusion coefficient of the majority charge carriers, N_t is the concentration of deep level impurities. Also, the a is the constant is determined from experimental data (I_1, V_1), (I_2, V_2) of the sections of injection depletion of the current-voltage curve.

$$a = Sln(U_2/U_1)/d(I_2 - I_1), \tag{8}$$

where S is the cross-sectional area. Authors of the research [19] contend that this happens when the exponent in expression (6) is greater than two ($J_{ad} > 2$). In this case $J_{ad}=9.27$ and the requirement is completely satisfied.

According to the authors of the research [20], such a section of the current-voltage characteristic is mainly observed as a result of ambipolar diffusion and drift migration of charge carriers. Ambipolar diffusion and drift processes often manifest themselves at higher concentrations of defects in deep levels inside the crystal lattice.

The above *XRD* and electron microscopy results suggest that the $ZnO_{1-x}S_x$ nanocrystals formed in *p-ZnO<S>/n-Si* heterostructures differ from substitutions of impurity atoms. These $ZnO_{1-x}S_x$ nanocrystals at the interface of blocks and near-surface regions represent deep impurities and are responsible for the observed part of the current-voltage characteristic.

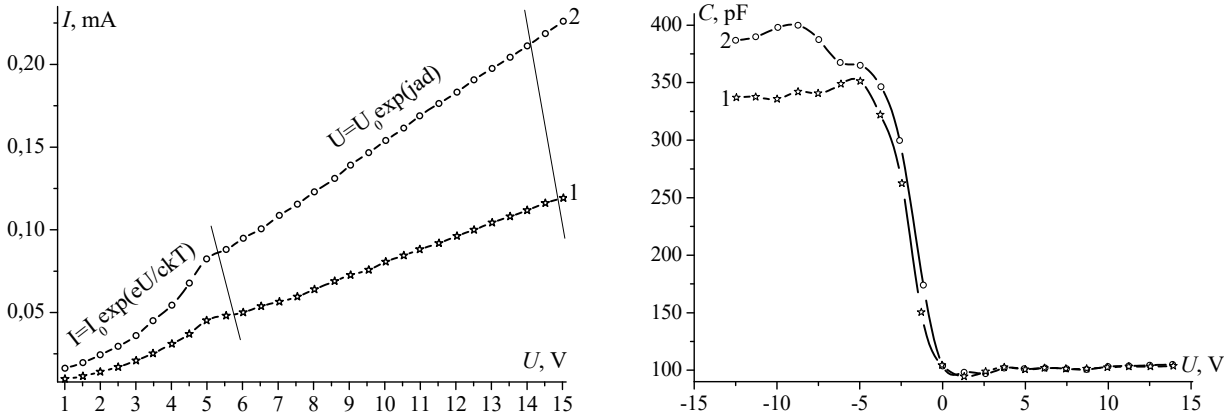

Figure 2. Current-voltage and capacitance-voltage characteristics of the *n-ZnO/p-Si* heterostructure before and after γ-irradiation

Capacitance-voltage characteristics were measured using a laboratory *CV*-meter, which had a source of adjustable *DC* bias voltage and a high-frequency (*500 kHz*) measuring signal of both polarities. The *CV* characteristics of the *p-ZnO<S>/n-Si* heterostructure before and after γ-irradiation were subsequently studied. The peak capacitance occurs in the region of negative voltages, which corresponds to the *p*-type conductivity of *ZnO<S>* films. Under the influence of γ-irradiation at doses of $5 \cdot 10^6$ *rad*, the capacitance of the heterostructure at negative voltages does increase, while at positive voltages, the capacitance of the heterostructure practically remains constant and negligent *(~110 pF)*. The *CV* curve of the heterostructure exhibits shelves and peaks along the *U* voltage axis. Such a behavior of high-frequency *CV* characteristics is indicative of the presence of a monoenergetic level of fast surface states at the heterointerface.

CONCLUSION

Thus, metal oxide layers of *p-ZnO<S>* were engineered on silicon substrates using the ultrasonic spray pyrolysis technique.

The resulting *ZnO<S>* films on silicon substrates had crystallographic orientations (*001*) and crystal lattice parameters $a = b = 0.3265$ nm and $c = 0.5212$ nm. $ZnO_{1-x}S_x$ nanocrystals on the film surface had sizes ranging from 57 nm to 200 nm. The lattice parameter of $ZnO_{1-x}S_x$ nano-crystallites was found experimentally to be $a_{ZnO<S>} = 0.7598$ nm.

It has been established that the lattice parameters of the *ZnO<S>* film and the geometric dimensions of $ZnO_{1-x}S_x$ nano-crystallites on the film surface decrease under the influence of *γ*-irradiation. It was also determined that the crystal structure of $ZnO_{1-x}S_x$ nano-crystallites corresponds to a cubic lattice and belongs to the space group *F43m.* The medium size of $ZnO_{1-x}S_x$ nano-crystallites were calculated and were found to be in the range of 10÷150 nm.

It was determined that after *γ*-irradiation at doses of $5 \cdot 10^6$ *rad*, the values of resistivity $\rho = 12.7$ Ω·cm and the mobility of the majority charge carriers $\mu = 0.18$ $cm^2/V \cdot s$ of *ZnO<S>* films had actually decreased, whereas their concentration had increased up to $N = 2{,}64 \cdot 10^{18}$ cm^{-3}.

The study of the current-voltage characteristics of *p-ZnO<S>/n-Si* heterostructures before and after *γ*-irradiation at doses of $5 \cdot 10^6$ *rad* had shown that the dependence of the current on voltage obeys an exponential law, which was described in the theory of the injection depletion phenomenon.

It has been determined that under the influence of *γ*-irradiation at doses of $5 \cdot 10^6$ *rad*, the capacitance of the *p-ZnO<S>/n-Si* heterostructure at negative voltages increases and the shelves and peaks are observed on the curve that might be associated with the presence of a monoenergetic level of fast surface states at the heterointerface.

Conflict of Interests

The authors declare that they have no conflict of interests

Funding

The present research work was financed under the project FZ-292154210 granted by the Ministry of Innovative Development of the Republic of Uzbekistan

ORCID

Sirajidin S. Zainabidinov, https://orcid.org/0000-0003-2943-5844; **Akramjon Y. Boboev**, https://orcid.org/0000-0002-3963-708X
Nuritdin Y. Yunusaliyev, https://orcid.org/0000-0003-3766-5420

REFERENCES

[1] M. Staszuk, D. Pakuła, Ł. Reimann, M. Król, M. Basiaga, D. Mysłek, and A. Kříž, "Structure and Properties of ZnO Coatings Obtained by Atomic Layer Deposition (ALD) Method on a Cr-Ni-Mo Steel Substrate Type," Materials (Basel), **13**(19), 4223 (2020). https://doi.org/10.3390%2Fma13194223

[2] A.N. Georgobiani, A.N. Gruzintsev, V.T. Volkov, and M.O. Vorobev, "Effect of annealing in oxygen radicals on the luminescence and electrical conductivity of ZnO:H films," Semiconductors, **36**(3), 284-288 (2002). https://doi.org/10.1134/1.1461400

[3] M. Li, Y. Liu, Y. Zhang, X. Han, T. Zhang, Y. Zuo, C. Xie, et al., "Effect of the Annealing Atmosphere on Crystal Phase and Thermoelectric Properties of Copper Sulfide," ACS Nano, **15**(3), 4967-4978 (2021). https://doi.org/10.1021/acsnano.0c09866

[4] Sh. Yuldashev, S. Zainabidinov, and N. Yunusaliev, "Ultrasonic production technology and properties of ZnO<S> films," Scientific Bulletin Physical and Mathematical Research, 2, 60-64 (2022). (in Russian)

[5] S. Zainabidinov, S. Rembeza, E. Rembeza, et al., "Prospects for the use of metal-oxide semiconductors in energy converters," Applied Solar Energy, **55(**1), 5–7 (2019). https://doi:10.3103/S0003701X1901014

[6] H. Beigli, M. Shaddoust, M.H. Ahmadi, and A. Khatibani, "Effect of low and relatively long-term gamma irradiation on physical properties of ZnO and ZnO:Co thin films," **108**, 798–808 (2023). https://doi.org/10.1007/s10971-023-06229-0

[7] M. Duinong et al., "Effect of Gamma Radiation on Structural and Optical Properties of ZnO and Mg-Doped ZnO Films Paired with Monte Carlo Simulation," Coatings. **12**(10), 1590 (2022). https://doi.org/10.3390/coatings12101590

[8] S. Zainabidinov, Sh. Utamuradova, and A. Boboev, "Structural Peculiarities of the $(ZnSe)_{1-x-y}(Ge_2)_x(GaAs_{1-\delta}Bi_\delta)_y$ Solid Solution with Various Nanoinclusions," Journal of Surface Investigation: X-ray, Synchrotron and Neutron Techniques, **16**, 1130-1134 (2022). https://doi.org/10.1134/S1027451022060593

[9] S.K. Guba, and V.N. Yuzevich, "Calculation of surface characteristics and pressure of InAs quantum dots in the GaAs matrix," Semiconductors, **48**(7), 932-937 (2014).

[10] Kimberly A Dick et al. "Control of III–V nanowire crystal structure by growth parameter tuning," Semicond. Sci. Technol. **25**, 024009 (2010). https://doi.org/10.1088/0268-1242/25/2/024009

[11] S. Zainabidinov, A. Saidov, A. Boboev, and J. Usmonov, "Features of the Properties of the Surface of $(GaAs)_{1-x-y}(Ge2)_x(ZnSe)_y$ Semiconductor Solid Solution with ZnSe Quantum Dots," Journal of Surface Investigation: X-ray, Synchrotron and Neutron Techniques, **15**(1), 94–99 (2021). https://doi.org/10.1134/S102745102101016X

[12] P. Abraham, S. Shaji, D. Avellaneda, J.A. Aguilar-Martínez, and B. Krishnan, "(002) oriented ZnO and ZnO:S thin films by direct ultrasonic spray pyrolysis: A comparative analysis of structure, morphology and physical properties," Materials Today Communications, **35**, 105909 (2023). https://doi.org/10.1016/j.mtcomm.2023.105909

[13] H. Kim, A. Piqué, J. Horwitz, H. Murata, Z. Kafafi, C. Gilmore, and D. Chrisey, "Effect of aluminum doping on zinc oxide thin films grown by pulsed laser deposition for organic light-emitting devices," Thin Solid Films, **377–378**, 798–802 (2000). https://doi.org/10.1016/S0040-6090(00)01290-6

[14] X. Zi-qiang, D. Hong, L. Yan, and C. Hang, "Al-doping effects on structure, electrical and optical properties of c-axis-orientated ZnO:Al thin films," Mater. Sci. Semicond. Proc. **9**, 132 (2006). https://doi.org/10.1016/j.mssp.2006.01.082

[15] P.K. Khabibullaev, Sh.U. Yuldashev, and R.A. Nusretov, "Electroluminescence of ZnO-based p-i-n structures fabricated by the ultrasound-spraying method," Doklady Physics, **52**, 300-302 (2007). https://doi.org/10.1134/S102833580706002X

[16] D. Oeba, J. Bodunrin, and S. Moloi, "The electrical characteristics and conduction mechanisms of Zn doped silicon-based Schottky barrier diode," Heliyon, **9**(12), 3-4 (2023). https://doi.org/10.1016/j.heliyon.2023.e22793

[17] I. Sapaev, and D. Babajanov, "Current-voltage characteristic of the injection photodetector based on M(In)–nCdS–pSi–M(In) structure". Semiconductor physics, **22**(2), 188-192 (2019). https://doi.org/10.15407/spqeo22.02.188

[18] J. Yan, Y. Chen, X. Wang, Y. Fu, J. Wang, J. Sun, G. Dai, Sh. Tao, and Y. Gao, "High-performance ultraviolet photodetectors based on CdS/CdS:SnS_2 superlattice nanowires," Nanoscale, **8**(30), 14580–14586 (2016). https://doi.org/10.1039/c6nr02915a

[19] A. Leiderman, S. Zainabidinov, and A. Boboev, "Current-voltage (I-V) characteristics of n-GaAs-p-$(GaAs)_{1-x-y}(ZnSe)_x(Ge_2)_y$ heterostructures," in: *The International Symposium "New Tendencies of Developing Fundamental and Applied Physics: Problems, Achievements, Prospectives*" (Tashkent, 2016), pp. 176-178.

[20] S.Z. Zainabidinov, and A.Y. Boboev, "Photoelectric Properties of n-ZnO/p-Si Heterostructures," Applied Solar Energy, **57(**6) 475-479 (2021). https://doi.org/10.3103/S0003701X21060177

ВПЛИВ γ-ОПРОМІНЮВАННЯ НА СТРУКТУРУ ТА ЕЛЕКТРОФІЗИЧНІ ВЛАСТИВОСТІ ПЛІВОК ZnO, ЛЕГОВАНИХ S

Сіражідін С. Зайнабідінов[a], Акрамжон Ю. Бобоєв[a,b], Нурітдін Ю. Юнусалієв[a]

[a]Андижанський державний університет імені З.М. Бабур, Андижан, Узбекистан

[b] Інститут фізики напівпровідників та мікроелектроніки Національного університету Узбекистану, 100057, Ташкент, Узбекистан, вул. Янги Алмазар, 20

Отримані плівки ZnO<S> характеризували кристалографічною орієнтацією (001) і параметрами ґратки a = b = 0,3265 нм і c = 0,5212 нм. Нанокристаліти $ZnO_{1-x}S_x$ на поверхні плівки мали характерні розміри від 50 нм до 200 нм. Параметр ґратки нанокристалітів $ZnO_{1-x}S_x$ експериментально визначено aZnO<S> = 0,7598 нм. Дослідження пролило світло на те, що відбувається з параметрами ґратки плівки ZnO та геометричними розмірами нанокристалітів $ZnO_{1-x}S_x$ на поверхні плівки під впливом гамма-опромінення. Встановлено, що кристалічна структура нанокристалітів $ZnO_{1-x}S_x$ являє собою кубічну решітку і належить до просторової групи F43m. Встановлено, що після γ-опромінення в дозах 5·106 рад питомий опір плівок ZnO<S> знижується до ρ = 12,7 *Ω*см, а рухливість основних носіїв заряду (μ) стає 0,18 $см^2$/В. ·s, а їх концентрація (N) зросла і становила 2,64·1018 $см^{-3}$. Дослідження вольт-амперних характеристик гетероструктур p-ZnO<S>/n-Si до та після γ-опромінення в дозах $5·10^6$ рад показало, що залежність струму від напруги має експоненціальний закон, який узгоджується з теорія явища виснаження ін'єкції. Встановлено, що під дією γ-опромінення в дозах $5·10^6$ рад ємність гетероструктури p-ZnO<S>/n-Si при від'ємних напругах збільшується і на кривій спостерігаються поличкові ділянки та піки. завдяки наявності моноенергетичного рівня швидких поверхневих станів на гетеропереході.

Ключові слова: *плівка; ультразвуковий розпилювальний піроліз; нанокристаліт; γ-опромінення; кристалографічна орієнтація; параметр решітки; носії заряду; ін'єкційне виснаження*